ORGANOMETALLICS

Article

pubs.acs.org/Organometallics

Catalytic Addition of Alcohols to Carbodiimides Mediated by Benzimidazolin-2-iminato Actinide Complexes

Heng Liu,[†] Natalia Fridman,[†] Matthias Tamm,[*,‡] and Moris S. Eisen[*,†]

[†]Schulich Faculty of Chemistry, Technion − Israel Institute of Technology, Haifa City 32000, Israel

[‡]Institut für Anorganische und Analytische Chemie, Technische Universität Braunschweig, Hagenring 30, 38106 Braunschweig, Germany

Supporting Information

ABSTRACT: The synthesis of methyl and methoxy substituted benzimidazolin-2-iminato actinide (IV) complexes (**1**−**4**), [(Bim$^{2\text{-MeOPh/Me}}$N)AnN″$_3$] and [(Bim$_{5\text{-Me}}^{\text{Dipp/Me}}$N)-AnN″$_3$] (An = U, Th; N″ = N(SiMe$_3$)$_2$), was performed by the protonolysis of the actinide metallacycles with the respective neutral benzimidazolin-2-imine ligand precursors. Full characterization, including X-ray diffraction studies for all the complexes, is reported. Despite the high oxophilicity of the actinide metal centers, these complexes displayed extremely high activities in the catalytic addition of aliphatic and aromatic alcohols to carbodiimides, under very mild conditions, providing a facile and highly efficient strategy for the construction of carbon−oxygen bonds. Various kinds of diols and triols can also be used in this intermolecular insertion, representing a large substrate scope for the application of these organoactinide precatalysts.

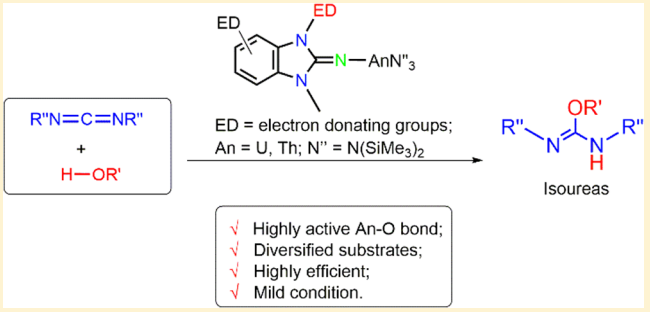

INTRODUCTION

Metal-catalyzed addition of O−H functionalities across carbon−carbon unsaturated bonds is a promising method for the construction of carbon−oxygen linkages. Some representative examples are the transition metal and lanthanide catalyzed hydroalkoxylation across alkenes and alkynes;[1−16] however, for these transformations, the catalytic reactivities and selectivities are highly dependent on the structural and electronic nature of the substrates, and sometimes the formation of byproducts is inevitable. Therefore, exploring novel selective and atom-economical catalytic systems, which can be also performed under relatively mild reaction conditions and generate negligible amounts of side products, is highly desirable. From the synthetic point of view, besides hydroalkoxylation of carbon−carbon unsaturated bonds, hydroalkoxylation of carbon−heteroatom multiple bonds, as present for instance in carbodiimides, can be treated as an alternative approach for the formation of carbon−oxygen bonds (Scheme 1(i)). Moreover, the produced isoureas are very important synthons in organic transformations and have been widely used as selective alkylating reagents.[17] Intriguingly, despite the intensive research on the addition of different nucleophiles E−H (E = N, P, ≡C) to carbodiimides,[18−23] a very limited number of systems are available to catalyze the addition of alcohols to carbodiimides,[24] which raised our curiosity in exploring such a catalytic process using organoactinide complexes.

In the past three decades, we have witnessed remarkable advances in the field of organoactinide catalysis, impelled initially by the distinctive characteristics of the actinide metal

Scheme 1. (i) Catalytic Addition of Alcohols to Carbodiimides and (ii) Mesomeric Structures of Benzimidazolin-2-iminato Ligands and the Corresponding Complexes

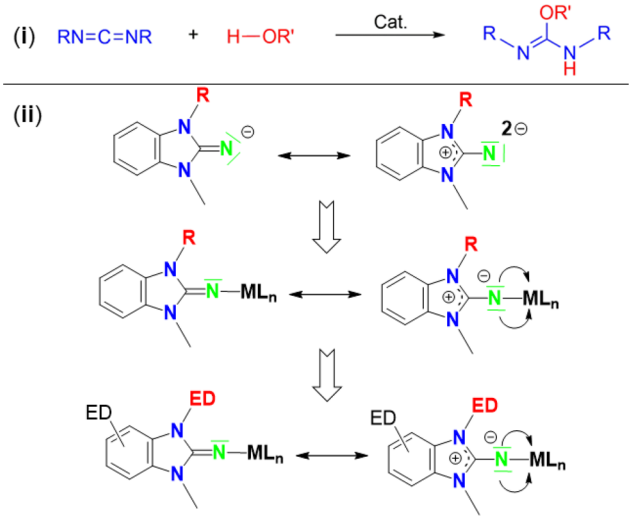

Special Issue: Organometallic Actinide and Lanthanide Chemistry

Received: June 11, 2017

DOI: 10.1021/acs.organomet.7b00432
Organometallics XXXX, XXX, XXX−XXX

centers, such as sizable ionic radii and unusual coordination numbers bringing unique geometries, and more recently by their capabilities in constructing carbon−carbon or carbon−heteroatom bonds. Hydroelementations,[25−32] coupling reactions,[33−37] olefin/diene polymerizations,[38−40] small-molecule activations,[41−48] etc. embrace some of these advances. However, most of these reactions excluded oxygenated substrates, due to the high oxophilicity of the actinide metals, which will usually form strong metal−oxygen bonds leading to partial deactivation of the active species.[14,49−53] Therefore, developing new generations of catalytic systems, which are capable of transforming oxygenated substrates, has been a long-standing subject. Some exciting breakthroughs have been made in very recent years. Being supported by highly nucleophilic, strongly basic donor ligands, such as cyclopentadienyl, amidinate, and imidazolin-2-iminato ligands, organoactinide complexes can be successfully employed in aldehyde dimerization (Tishchenko reaction),[54−57] hydroalkoxylation/cyclization of alkynyl alcohols,[58] and cyclic ester/epoxide ring-opening polymerizations.[59−64] These impressive results innovated the understanding of actinide catalysis and revealed that actinide−oxygen (An−O) bonds can be catalytically active to some extent, despite of their high bond energies (Th−O = 208.0, U−O = 181.0 kcal mol^{-1}).[65] Inspired by these findings, uranium- and thorium-based complexes were applied toward the intermolecular addition of alcohols to carbodiimides. Exploratory investigation employing sterically accessible actinide−amido complexes shows that the addition products, isoureas, can be obtained in high yields under very mild conditions;[66] however, the exact structure of the active species was inconclusive due to the formation of a mixture of actinide alkoxides, which usually had poor solubilities in hydrocarbon solvents.[67,68] A great improvement has been achieved by using benzimidazolin-2-iminato-supported actinide complexes, which not only displayed high activities in the hydroalkoxylation because of the sterically accessible nature of the actinide center but also allowed us to elucidate the structure of active species due to the enhanced solubility provided by the benzimidazolin-2-iminato complexes.[69] Nevertheless, when we exposed these benzimidaozlin-2-iminato actinide complexes to an excess of alcohol at high temperature (50 °C), cleavage of the actinide−nitrogen (An−N) bonds was observed, despite of the high bond order resulting from the ability of the imidazolin-2-iminato ligand to act as a strong 2σ,4π-electron donor (Scheme 1(ii)).[70] In order to enhance the thermal stability of the benzimidazolin-2-iminato complexes, various electron-donating groups were introduced to the backbone, based on the consideration that these groups might further increase the electron-donating ability of the ligands and therefore the stability of the resulting An−N bonds. A detailed study of the catalytic performance of the corresponding complexes is also presented herein.

RESULTS AND DISCUSSION

Synthesis and Structure Characterization. Benzimidazolin-2-imines with electron-donating groups (OMe (**a**), Me (**b**)) were synthesized according to Scheme 2. Coupling reaction between nitro-substituted aryl halides and substituted anilines afforded **a1** and **b1**, which were then reduced, followed by ring closure to give rise to the ligand precursor **a2** and **b2** in high yields. Methylation of **a2** and **b2** using methyl triflate and subsequent deprotonation with KH furnished the target ligands, **a** and **b**. The reaction of these neutral ligands with an equimolar

Scheme 2. Synthetic Procedures for Ligands a and b and Complexes 1−4

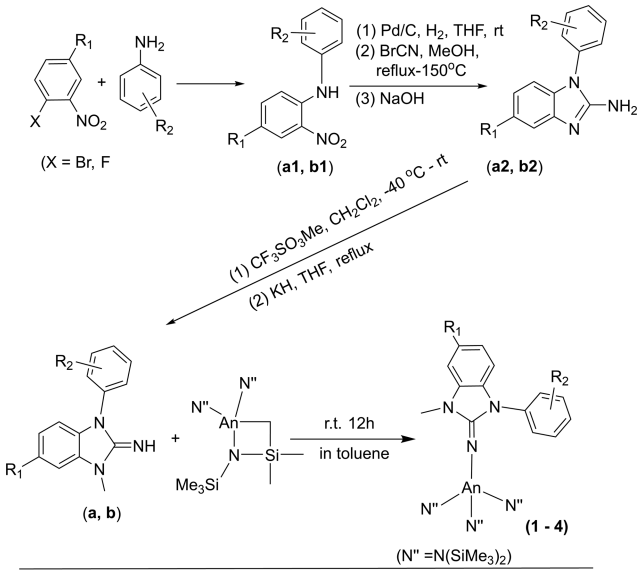

	a	b	1	2	3	4
R_1	H	5-Me	H	H	5-Me	5-Me
R_2	2-OMe	2,6-^{i}Pr$_2$	2-OMe	2-OMe	2,6-^{i}Pr$_2$	2,6-^{i}Pr$_2$
An	--	--	U	Th	U	Th

amount of the actinide metallacycles, $[(Me_3Si)_2N]_2An[\kappa^2$-$(N,C)$-$CH_2Si(CH_3)_2N(SiMe_3)]$ (An = Th, U), at room temperature for 24 h and recrystallization from a concentrated toluene solution afforded the benzimidazolin-2-iminato actinide complexes (**1**−**4**), in high yields. When compared with ^{1}H NMR spectra of the free ligands, complete disappearance of characteristic N*H* broad singlets at δ = 4.51 ppm (**a**) and 4.33 ppm (**b**) can be easily observed, indicating the formation of the corresponding actinide complexes.

Complexes **1**−**4** showed high instability and decomposed immediately at room temperature when exposed to air and moisture. To determine the crystal structures of these complexes, the single crystalline materials were submerged in cold (−35 °C) perfluoropolyalkylether oil in a vial, and subsequently submerged in liquid nitrogen, and the single crystals were fished from the vial at −78 °C and rapidly mounted on the diffractometer, receiving a cold jet of liquid nitrogen. The solid structures of the benzimidazolin-2-iminato uranium(IV) and thorium(IV) complexes, $[(Bim^{2\text{-}MeOPh/Me}N)UN''_3]$ (**1**) and $[(Bim^{2\text{-}MeOPh/Me}N)ThN''_3]$ (**2**), are shown in Figure 1; both complexes display a distorted tetrahedral geometry around the metal center, which is built by four nitrogen atoms. Despite of the highly oxophilic nature of the actinide centers, neither intermolecular nor intramolecular interactions between the methoxy group and the U/Th atom was observed. Like in other imidazolin-2-iminato actinide complexes, the An−$N_{C=N}$ bond distances (2.105(5), 2.171(6) Å, for complexes **1** and **2**, respectively) are on average 0.2 Å shorter than the An−N_{amido} bonds in the same complexes, indicative of the higher bond order of the benzimidazolin-2-iminato ligand to the metal center. The An−N(1)−C(1) angles are close to linearity, displaying values of 165.7(4)° and 164.0(4)° for complexes **1** and **2**, respectively. It is worthy of

DOI: 10.1021/acs.organomet.7b00432
Organometallics XXXX, XXX, XXX−XXX

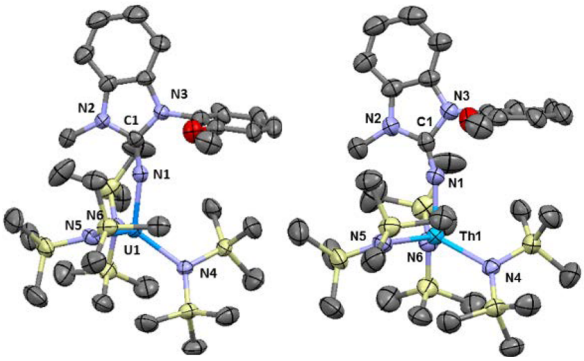

Figure 1. ORTEP drawings of complexes **1** (left) and **2** (right) with thermal displacement parameters at 50% probability. Hydrogen atoms are omitted for clarity. Bond lengths (Å): An−N1 2.105(5), 2.171(6); An−N4 2.317(4), 2.383(6); An−N5 2.286(4), 2.344(10); An−N6 2.312(5), 2.359(6); C1−N1 1.297(7), 1.275(8). Bond angles (deg): An−N1−C1 165.7(4), 164.0(4); N1−An−N4 118.70(17), 115.9(2); N1−U−N5 92.30(16), 92.95(18); N1−An−N6 100.17(17), 101.1(2); N4−An−N5 116.87(16), 101.1(2); N4−An−N6 108.81(16), 108.7(2); N5−An−N6 118.34(17), 118.6(2). All the values are first for complex **1** and then for complex **2**.

note that these values are on average slightly smaller than those in the corresponding imidazolin-2-iminato actinide complexes (169.5(5)° and 170.7(7)°) decorated with symmetrical ligands.[57] This difference can be ascribed to the asymmetric nature of the benzimidazolin-2-iminato ligand, with the bulkier diisopropylphenyl group repelling the adjacent $N(SiMe_3)_2$ substituents and subsequently pushing the An−N(1) bond toward the sterically more open side of the smaller methyl group. To describe the proximity of the ligand to the metal center, cone angles were determined.[71] The resulting cone angles for complexes **1** and **2** are 136.5° and 132.7°, respectively, which are much smaller than the cone angles in imidazolin-2-iminato actinide complexes (204°, 206°),[57] indicating a more open space around the metal center herein. For all the complexes, no agostic interaction between the $-N(SiMe_3)_2$ or the isopropyl groups and the actinide metal was observed.

Single crystal structures of the methyl substituted benzimidazolin-2-iminato uranium(IV) and thorium(IV) complexes, $[(Bim_{5\text{-}Me}{}^{Dipp/Me}N)UN''_3]$ (**3**) and $[(Bim_{5\text{-}Me}{}^{Dipp/Me}N)UN''_3]$ (**4**), are shown in Figure 2, and similarly to complexes **1** and **2**, distorted tetrahedral geometries around the metal center were observed. Moreover, in both complexes, shorter $An-N_{C=N}$ bond as well as approximate linearity of the An−N(1)−C(1) bond angle are displayed, with values of 2.131(3) Å, 163.2(3)° for complex **3** and 2.206(3) Å, 161.5(2)° for complex **4**, respectively. Due to the bigger size of Dipp than 2-MeOPh (in complexes **1** and **2**), larger An−N−C bend angles are found in complexes **3** and **4**.

Catalytic Insertion of Alcohols into Carbodiimides. The results for catalytic addition of various kinds of alcohols to 1,3-di-*p*-tolylcarbodiimide (DTC) are presented in Table 1. The reaction of methanol and DTC was first investigated by using the different catalysts (**1**−**4**) at room temperature, and all the complexes exhibited high activities during the catalytic process, affording the isourea products almost quantitatively within 1 h, indicating the high efficiencies of the four complexes (Scheme 3). It is important to note that no detectable products were observed in the corresponding blank reactions without the actinide complexes.

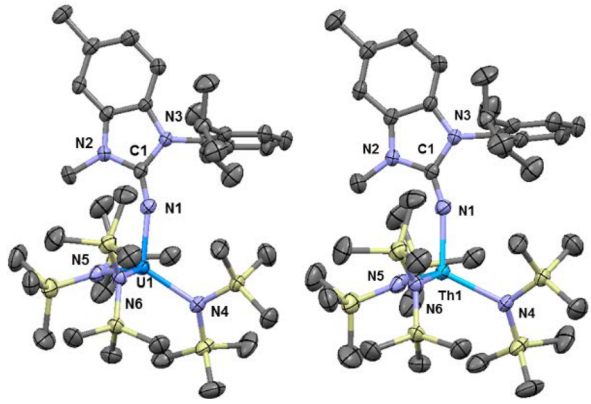

Figure 2. ORTEP drawings of complexes **3** (left) and **4** (right) with thermal displacement parameters at 50% probability. Hydrogen atoms are omitted for clarity. Bond lengths (Å): An−N1 2.131(3), 2.206(3); An−N4 2.313(3), 2.389(3); An−N5 2.290(3), 2.360(5); An−N6 2.293(3), 2.355(4); C1−N1 1.279(5), 1.279(4). Bond angles (deg): An−N1−C1 163.2(3), 161.5(2); N1−An−N4 117.74(13), 115.32(10); N1−U−N5 95.11(13), 95.87(12); N1−An−N6 104.61(13), 105.52(13); N4−An−N5 116.50(12), 116.43(11); N4−An−N6 107.58(12), 107.90(11); N5−An−N6 114.61(13), 115.08(15). All the values are first for complex **3** and then for complex **4**.

Table 1. Catalytic Addition of Various Alcohols to DTC[a]

entry	cat.	R′−OH	time (h)	yield (%)	product
1	**1**	MeOH	1	>99	**5a**
2	**2**		1	>99	
3	**3**		1	>99	
4	**4**		1	>99	
5	**1**	EtOH	1	>99	**5b**
6	**2**		1	>99	
7	**1**	^{i}PrOH	1	96	**5c**
8	**2**		1	97	
9	**1**	^{t}BuOH	12	70	**5d**
10	**2**		12	86	
11	**1**	BnOH	1	>99	**5e**
12	**2**		1	>99	
13	**1**	Py-2-CH_2OH	1	>99	**5f**
14	**2**		1	>99	
15	**1**	Thio-2-CH_2OH	1	>99	**5g**
16	**2**		1	>99	
17	**1**	Furan-2-CH_2OH	1	>99	**5h**
18	**2**		1	>99	
19	**1**	CyOH	4	>99	**5i**
20	**2**		4	>99	
21	**1**	Ph_2CHOH	12	84	**5j**
22	**2**		12	86	
23	**1**	1-Adamantanol	6	>99	**5k**
24	**2**		6	>99	
25	**1**	PhOH	1	>99	**5l**
26	**2**		1	>99	
27	**1**	2,6-Me_2PhOH	1	92	**5m**
28	**2**		1	95	
29	**1**	2,4-^{t}BuPhOH	12	77	**5n**
30	**2**		12	83	

[a]Reaction conditions: 2 mol % precatalyst, 50 equiv of substrates (0.35 mmol), 500 μL of C_6D_6, room temperature. The yields were determined by ^{1}H NMR of the crude reaction mixture.

DOI: 10.1021/acs.organomet.7b00432
Organometallics XXXX, XXX, XXX−XXX

Scheme 3. Catalytic Addition of Alcohols to DTC

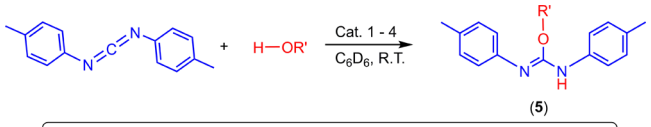

R'OH = MeOH (**a**), EtOH (**b**), ^{i}PrOH (**c**), ^{t}BuOH (**d**), BnOH (**e**), Py-2-CH_2OH (**f**), Thio-2-CH_2OH(**g**), Furan-2-CH_2OH (**h**), CyOH (**i**), Ph_2CHOH(**j**), 1-Adamantanol (**k**) PhOH (**l**), 2,6-Me_2PhOH (**m**), 2,4-$^{t}Bu_2$PhOH (**n**),

Complexes **1** and **2** were then chosen as precatalysts to study the scope of this intermolecular coupling. Table 1 shows that a wide range of primary, secondary, and tertiary alcohols can be used for this reaction. Increasing the size of the alcohol from MeOH to EtOH or to ^{i}PrOH showed a modest influence on the yield of the insertion products, and all of them were almost quantitatively converted to the corresponding isoureas in the same period of time at room temperature. However, further increasing the size of the alcohol to ^{t}BuOH resulted in a drastic slowdown of the reaction rate, and only 70% and 86% conversion was observed after 12 h for complexes **1** and **2**, respectively. This result indicates the reduced accessibility of the carbodiimide to the actinide center due to the sterically demanding *tert*-butyl group. Similarly, when other tertiary alcohols such as diphenylmethanol or 1-adamantanol as the nucleophiles were used, much longer reaction times were required to completely consume the starting material (runs 21−24, Table 1).[66] Interestingly, the use of heteroatomic alcohols (runs 13−18), that is, 2-pyridinemethanol, 2-thiophenemethanol, or 2-furanmethanol, did not reduce the activity of the complexes, which proceeded to completion within an hour. Compared with actinide amido mediated systems, the present two complexes performed with higher activities due to the presence of the benzimidazolin-2-iminato ligand. In this sense, the ligand will lead to a reduced electrophilicity on the metal center and therefore an expected increase in its catalytic reactivity.[66] In addition, the presence of the ligand improves the solubility of the alkoxo active species in benzene. Interestingly, in the catalytic addition of alcohols to 1,3-di-*p*-tolylcarbodiimide, a lower reactivity is obtained when using the metallacycle thorium amido complex $[(Me_3Si)_2N]_2Th[\kappa^2\text{-}(N,C)\text{-}CH_2Si(CH_3)_2N(SiMe_3)]$, due to the formation of insoluble actinide alkoxides moieties.[66]

Phenols of different size were also investigated as substrates for the intermolecular coupling (entries 25−30, Table 1). Similar to the aliphatic alcohols, less bulky phenol (PhOH) and 2,6-dimethylphenol (2,6-Me_2PhOH) react with DTC furnishing the insertion products in high yields within an hour. For the more sterically encumbered 2,4-di-*tert*-butylphenol (2,4-$^{t}Bu_2$PhOH), a sluggish reactivity with moderate yields of 77% and 83% was observed after 12 h for complexes **1** and **2**, respectively. Figure 3 shows the progress of the reaction as a function of DTC/2,4-$^{t}Bu_2$PhOH consumption and isourea formation using complex **2**. The signals at 1.24 and 1.50 ppm were assigned to the *ortho*- and *para*-*tert*-butyl groups of the starting material 2,4-$^{t}Bu_2$PhOH, whereas the signals at 1.13 and 1.41 ppm were assigned to the corresponding *tert*-butyl groups of the addition product.

The reaction scope was next explored with a series of diarylcarbodiimides using 2 mol % of the actinide complexes **1** and **2** (Scheme 4 and Table 2). It was found that the carbodiimide substrates with higher steric encumbrance

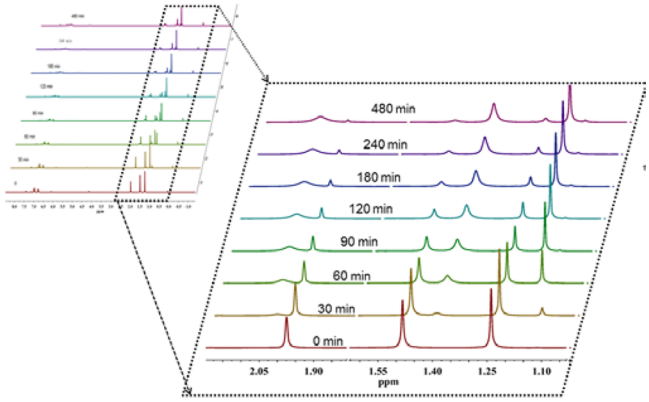

Figure 3. Reaction progress in the coupling of 2,4-di-*tert*-butylphenol and DTC catalyzed by complex **2**.

Scheme 4. Catalytic Addition of Methanol to Various Kinds of Carbodiimides

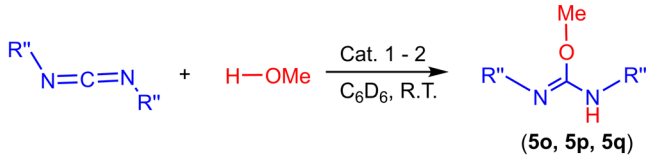

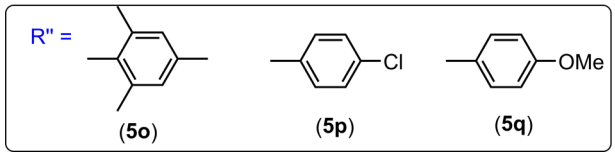

Table 2. Catalytic Addition of Methanol to Various Kinds of Carbodiimides (R″NCNR″)[a]

entry	cat.	R″	time (h)	yield (%)	product
1	**1**	Mes	1	>99	**5o**
2	**2**		1	>99	
3	**1**	4-ClPh	1	>99	**5p**
4	**2**		1	>99	
5	**1**	4-MeOPh	1	>99	**5q**
6	**2**		1	>99	

[a]Reaction conditions: 2 mol % precatalyst, 50 equiv of substrates (0.35 mmol), 500 μL of C_6D_6, room temperature. The yields were determined by ^{1}H NMR of the crude reaction mixture.

(MesNCNMes) or strongly electron-withdrawing groups ((4-ClPh)NCN(4-ClPh)) or strongly electron-donating groups ((4-MeOPh)NCN(4-MeOPh)) are able to undergo efficient insertion to afford the corresponding isoureas in high yields within 1 h. Note that changing the metal center showed little influence on the catalytic behaviors, and both uranium (**1**) and thorium (**2**) complexes displayed high activities in this process.

In order to expand the scope of the precatalysts **1** and **2** and to synthesize polyfunctionalized compounds with the potential to serve as templates for the construction of larger molecules, diols and triols were also investigated. In the presence of catalytic amounts of the complexes **1** and **2**, symmetric diols or triols reacted with DTC in a 1:2 or 1:3 molar ratio furnishing, in high yields, the corresponding diisourea and triisourea, respectively (Scheme 5). Reacting the nonsymmetric diol 1,3-butanediol in a 1:1 ratio with DTC with catalytic amounts of complex **2** afforded the monoisourea products **8a** and **8b** in a

DOI: 10.1021/acs.organomet.7b00432
Organometallics XXXX, XXX, XXX−XXX

Scheme 5. Catalytic Addition of Diols and Triols to DTC

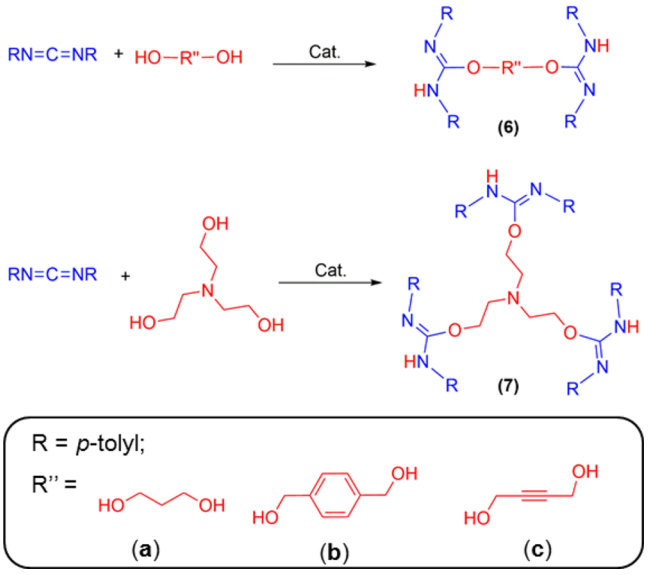

ratio of 1:1.7, respectively, revealing a higher reactivity for the primary alcohol moiety. Addition of another equivalent of DTC to this reaction mixture gave the diisourea **9** quantitatively (Scheme 6).

Scheme 6. Catalytic Addition of 1,3-Butanediol to DTC Catalyzed by Complex 2

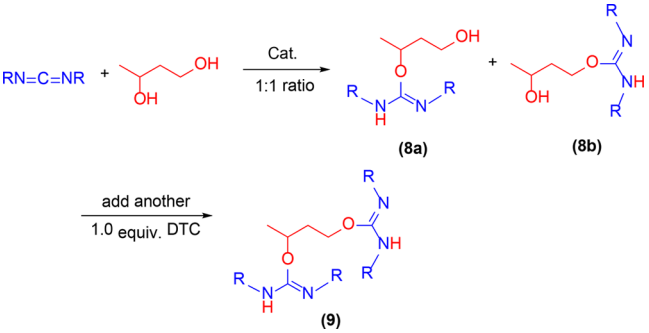

To elucidate the catalytically active species and to investigate their thermal stabilities, stoichiometric reactions of complex **4** with 10 equiv of 2,4-di-*tert*-butylphenol were carried out *in situ* in benzene-d_6. Upon addition, 3 equiv of hexamethyldisilazane were released immediately, affording the corresponding benzimidazolin-2-iminato thorium(IV) trialkoxide complex, [(Bim$_{5\text{-Me}}^{\text{Dipp/Me}}$N)Th(O-2,4-^{t}Bu$_2$Ph)$_3$]. To this reaction mixture, 10 equiv of DTC were added, and the rapid appearance of the isourea product was observed. In contrast, leaving the mixture of complex **4** with 10 equiv of DTC at room temperature for 24 h did not afford any addition of the amido groups to the carbodiimide, indicating that the actinide trialkoxide complexes serve as a truly active species during the catalytic cycle. Exposing the methylated benzimidazolin-2-iminato thorium(IV) trialkoxide complex [(Bim$_{5\text{-Me}}^{\text{Dipp/Me}}$N)-Th(O-2,4-^{t}Bu$_2$Ph)$_3$] to an excess of 2,4-di-*tert*-butylphenol at 50 °C induced the protonolysis of the ligand.[69] However, for the methoxylated benzimidazolin-2-iminato thorium(IV) trialkoxide species [(Bim$^{\text{2-MeOPh/Me}}$N)Th(O-2,4-^{t}Bu$_2$Ph)$_3$], the presence of an excess amount of 2,4-di-*tert*-butylphenol at 50 °C for 12 h, did not induce any decomposition. Protonolysis of the complex starts at 80 °C, indicating that the introduction of the methoxy group can only partially increase the stability of the active species.

Kinetic studies for the catalytic addition of 2,4-di-*tert*-butylphenol to DTC employing precatalyst **2** were next conducted by changing one substrate or catalyst while keeping the other reagents constant, and the progress of the reaction was monitored by in situ ^{1}H NMR spectroscopy. As shown in Figures 4–6, the rate of product formation displays a first-order

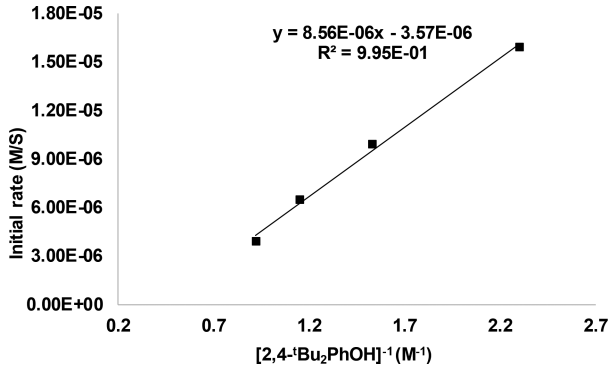

Figure 4. Plot of initial reaction rate against the inverse concentration of 2,4-di-*tert*-butylphenol (2,4-^{t}Bu$_2$PhOH).

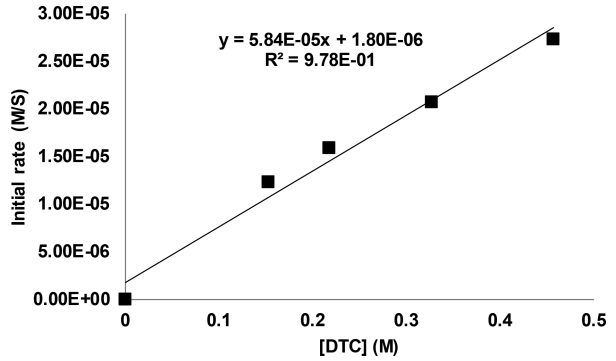

Figure 5. Plot of initial reaction rate against the concentration of DTC.

dependence on DTC and complex **2** and an inverse first-order dependence on 2,4-di-*tert*-butylphenol, giving rise to the kinetic eq 1 (detailed analysis of the kinetic equation can be found in the experimental section). The inverse first order indicates that an excess of alcohol coordinates to the active species **CatA**

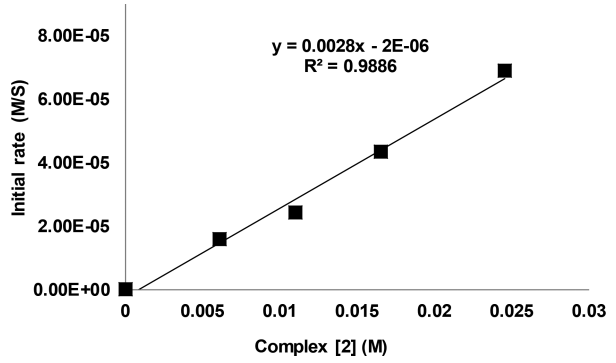

Figure 6. Plot of initial reaction rate against the concentration of precatalyst **2**.

DOI: 10.1021/acs.organomet.7b00432
Organometallics XXXX, XXX, XXX–XXX

(Scheme 6) taking it out of the catalytic cycle with the formation of the complex **C**.[72]

$$\frac{\partial p}{\partial t} = K_{obs}[2]^1[DTC]^1[^tBu_2PhOH]^{-1} \quad (1)$$

Thermodynamic activation parameters were determined from the Eyring (Figure 7) and Arrhenius plots, displaying a low

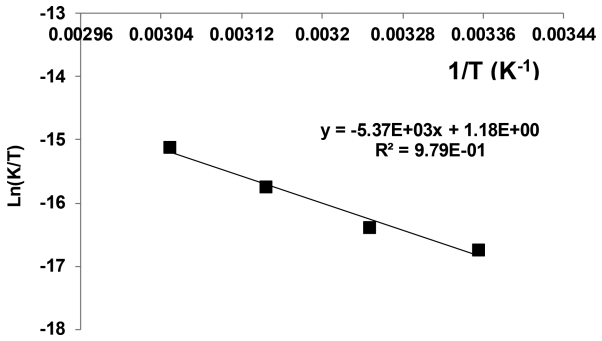

Figure 7. Eyring plot of 2,4-di-*tert*-butylphenol (2,4-^{t}Bu$_2$PhOH), DTC, and **2** system.

activation barrier (E_a) of 11.2(9) kcal mol^{-1}, and enthalpy ($\Delta H^{\ddagger}$) and entropy ($\Delta S^{\ddagger}$) of activation of 10.6(7) kcal mol^{-1} and −44.8(8) eu, respectively, indicating an ordered transition state during the rate-determining insertion step. Based on the above analysis, a plausible mechanism for the catalytic addition of alcohols to DTC is proposed in Scheme 7. In the first step,

Scheme 7. Plausible Mechanism for Catalytic Insertion of Alcohols into DTC

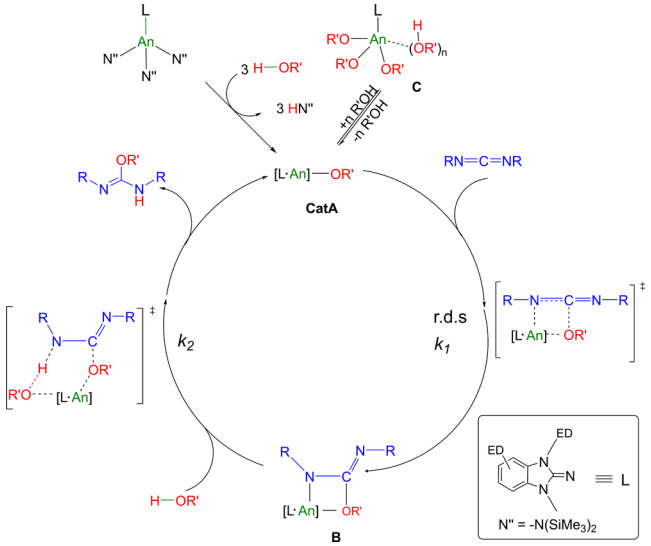

the active species, the benzimidazolin-2-iminato actinide alkoxide (**CatA**), is formed by protonolysis of the amido groups with the alcohol with the concomitant release of three equivalents of HN(SiMe$_3$)$_2$. **CatA** was characterized by NMR spectroscopy obtained from the stoichiometric reaction between complex **4** with 3 equiv of 2,4-^{t}Bu$_2$PhOH. Then **CatA** reacts with DTC, affording the actinide−isourea species **B**, which is subsequently protonated by another molecule of alcohol, furnishing the final isourea with regeneration of **CatA**. Deuterium labeling studies using 2,4-^{t}Bu$_2$PhOD, DTC, and complex **2** revealed a KIE value of K_H/K_D = 1.04, indicating that the protonolysis is a fast step and that the insertion of DTC into the actinide alkoxide moiety is the rate-determining step.

Regarding the yields of the reaction (Tables 1 and 2), it is important to note that when 2 mol % of the precatalyst is used, 6% of [LAn]−OR′ (intermediate **CatA**, Scheme 7) will be formed. At the end of the reaction, the precatalyst will finally remain as the actinide pre-isourea intermediate (intermediate **B**), rather than in the **CatA** form. For intermediate **B**, which only needs external protons to release the final product, the characteristic ^{1}H NMR always overlapped with the ^{1}H NMR of the final isourea products, which prevents us from differentiating them. Based on these considerations, we have calculated the ratio of the products (including intermediate **B** and the isourea products) and the starting material. In addition, quenching every reaction mixture with external proton resources released the 6% of the isourea from complex **B** affording yields of >99%.

CONCLUSION

The synthesis and characterization of methyl and methoxy substituted benzimidazolin-2-iminato actinide complexes (**1**−**4**) are reported herein. X-ray single crystal analysis revealed short An−N$_{C=N}$ bonds, indicative of a higher An−N$_{C=N}$ bond order. At room temperature, all four complexes showed high activities in catalyzing the addition of aliphatic and aromatic alcohols to carbodiimides. In addition, various diols and triols were also employed in this reaction. Kinetic studies revealed that the reaction follows a first-order dependence on precatalyst and carbodiimide and an inverse first-order on the alcohol. A plausible mechanism is proposed, in which the insertion of the carbodiimide into the actinide alkoxide species was found to be the rate-determining step.

EXPERIMENTAL SECTION

All manipulations of air sensitive materials were performed with rigorous exclusion of oxygen and moisture in flamed Schlenk-type glassware on a high vacuum line (10^{-5} Torr) or in nitrogen filled MBraun and Vacuum Atmospheres gloveboxes with a medium capacity recirculator (1−2 ppm oxygen). Argon and nitrogen were purified by passage through a MnO oxygen removal column and a Davison 4 Å molecular sieve column. Analytically pure solvents were dried and stored with Na/K alloy and degassed by three freeze−pump−thaw cycles prior to use (hexane, toluene, benzene-d_6). MeOH, EtOH, ^{i}PrOH, ^{t}BuOH, BnOH, 2-pyridinemethanol, 2-thiophenemethanol, 2-furanmethanol, CyOH, HO(CH$_2$)$_3$OH, and N-(CH$_2$CH$_2$OH)$_3$ were distilled under CaH$_2$ and stored over 4 Å molecular sieves. PhOH, 2,6-dimethylphenol (2,6-Me$_2$PhOH), 2,4-di-*tert*-butylphenol, Ph$_2$CHOH, 1-adamantanol, and 1,3-di-*p*-tolylcarbodiimide (Sigma-Aldrich) were dried for 12 h on a high vacuum line (10^{-5} Torr) and stored in a glovebox prior to use. The actinide metallacycles were prepared according to previous reports.[73] Deuterated 2,4-di-*tert*-butylphenol (2,4-^{t}Bu$_2$PhOD) was prepared using a similar method according to published procedures.[74] 1,3-Di-(2,4,6-trimethylphenyl)carbodiimide,[75] 1,3-di-*p*-chlorophenylcarbodiimide,[76] and 1,3-di-*p*-methoxylphenylcarbodiimide,[76] were prepared according to previous reports. 1-Fluoro-2-nitrobezene, *o*-anisidine, 4-bromo-3-nitrotoluene, 2,6-diisopropylaniline (97%), tris-(dibenzylideneacetone)dipalladium(0) (Pd$_2$(dpa)$_3$), (±)-2,2′-bis-(diphenylphosphino)-1,1′-binaphthalene (±BINAP), cesium carbonate (Cs$_2$CO$_3$), palladium on activated charcoal (Pd/C; 5% Pd), and methyl trifluoromethanesulfonate (CF$_3$SO$_3$CH$_3$) were purchased from Sigma-Aldrich and used as received.

DOI: 10.1021/acs.organomet.7b00432
Organometallics XXXX, XXX, XXX−XXX

NMR spectra were recorded on Bruker Avance 300 and Avance 400 spectrometers. Chemical shifts for ^{1}H and ^{13}C NMR measurements are reported in ppm and referenced to the residual proton or carbon signals of the deuterated solvents relative to tetramethylsilane. Elemental analyses were carried out by the microanalysis laboratory at the Hebrew University of Jerusalem. MS experiments were performed at 200 °C (source temperature) on a Maxis Impact (Bruker) mass spectrometer with an APCI solid probe method. For X-ray crystallographic measurements, the single crystals were immersed in perfluoropolyalkylether oil and quickly mounted on a Kappa CCD diffractometer under flow of liquid nitrogen. Data collection was performed using monochromated Mo Kα radiation using φ and ω scans to cover the Ewald sphere.[77] Accurate cell parameters were obtained with the amount of indicated reflections (Table S1).[78] The structure was solved by SHELXS-97 direct methods[79] and refined by the SHELXL-97 program package.[80] The atoms were refined anisotropically. Hydrogen atoms were included using the riding model. CCDC 1544404−1544407 for **1**−**4**.

Synthesis of 2-Methoxy-*N*-(2-nitrophenyl)aniline (a1). To a 100 mL round-bottom flask, 1-fluoro-2-nitrobezene (8.46 g, 60 mmol), *o*-anisidine (12.6 g, 100 mmol), and potassium fluoride (6.96 g, 120 mmol) were added. The reaction mixture was refluxed at 180 °C for 24 h. After cooling to room temperature, the mixture was washed with water (3 × 50 mL) and extracted with dichloromethane (3 × 50 mL), dried over $MgSO_4$, and concentrated under vacuum. Excess *o*-anisidine was removed by vacuum distillation, and then the crude product was purified by column chromatography on silica with the eluent of *n*-hexane/ethyl acetate (10/1), affording the target product **a1**, after evaporation of the solvent, as a yellow powder. Yield: 10.3 g (77%). ^{1}H NMR (400 MHz, $CDCl_3$) δ 9.36 (s, 1H, N*H*), 8.12 (m, 1H, H_{Ar}), 7.31−7.24 (m, 2H, H_{Ar}), 7.22−7.15 (m, 1H, H_{Ar}), 7.15−7.03 (m, 1H, H_{Ar}), 6.95−6.84 (m, 2H, H_{Ar}), 6.72−6.63 (m, 1H, H_{Ar}), 3.79 (s, 3H, CH_3). $^{13}C\{^{1}H\}$ NMR (101 MHz, $CDCl_3$) δ 152.56, 142.51, 135.44, 133.80, 127.88, 126.67, 125.77, 123.29, 120.68, 117.43, 116.22, 111.64, 55.72. MS (APCI): *m*/*z* 245.0310 $(M + H)^+$.

Synthesis of 1-(2-Methoxyphenyl)-3-methylbenzimidazolin-2-imine (a). To a 100 mL round-bottom flask, 2-methoxy-*N*-(2-nitrophenyl)aniline (2.0 g, 8.2 mmol), THF (30 mL), and 5% Pd/C (0.4 g) were added, and the flask was carefully placed under 1 atm H_2. The mixture was stirred vigorously overnight at room temperature (TLC was used to monitor the reduction process) and then filtered through a pad of Celite and concentrated, affording the diamine quantitatively. Then the flask was charged with cyanogen bromide (1.06 g, 10 mmol) and 30 mL of absolute ethanol, and the mixture was stirred at room temperature for 30 min and then refluxed for 2 h. To complete the reaction, the temperature was then increased to 150 °C for 1 h. The solvent was then removed completely under vacuum, and 50 mL of diethyl ether was added. The mixture was stirred for 30 min, and the resulting precipitate was filtered off, washed with diethyl ether, and then dissolved in 50 mL of $CHCl_3$. To this solution, 50 mL of 1 M NaOH aqueous solution was added, and the mixture was stirred for 2 h. The organic layer was collected, and the remaining aqueous phase was extracted with $CHCl_3$ (3 × 30 mL). The combined organic fraction was dried over $MgSO_4$ and concentrated *in vacuo* to afford 1-(2-methoxyphenyl)-1*H*-benzimidazol-2-amine (**a2**) as the final product. Yield: 1.67 g (85%). ^{1}H NMR (400 MHz, $CDCl_3$) δ 7.45−7.37 (m, 2H, H_{Ar}), 7.34−7.30 (m, 1H, H_{Ar}), 7.11−7.03 (m, 3H, H_{Ar}), 6.97−6.89 (m, 1H, H_{Ar}), 6.82−6.76 (m, 1H, H_{Ar}), 4.64 (s, 2H, N*H*), 3.74 (s, 3H, CH_3). $^{13}C\{^{1}H\}$ NMR (101 MHz, $CDCl_3$) δ 176.76, 154.93, 153.12, 149.21, 141.71, 135.26, 130.51, 128.95, 123.04, 121.78, 120.12, 117.47, 116.25, 112.82, 108.50, 55.35. MS (APCI): *m*/*z* 240.0994 $(M + H)^+$.

The precursor obtained above (2 g, 8.35 mmol) was redissolved in CH_2Cl_2 (30 mL), and the solution was cooled to −40 °C. $CF_3SO_3CH_3$ (1.1 equiv) was added dropwise, and the reaction mixture was stirred at this temperature for 1 h. The mixture was allowed to warm to room temperature and stirred overnight. After removal of the solvent *in vacuo*, the remaining solid was washed with diethyl ether (2 × 20 mL), dried *in vacuo*, and redissolved in 30 mL of THF. KH (0.38 g, 9.5 mmol) was added to the solution slowly (gas was evolved immediately), then the mixture was stirred at room temperature for 30 min and subsequently refluxed for 2 h. The solvent was completely removed, and 30 mL of diethyl ether was added to extract the target ligand. Filtration and evaporation afforded the final ligand (**a**) as a white powder. Yield: 1.93 g (91%). ^{1}H NMR (400 MHz, $CDCl_3$) δ 7.45−7.35 (m, 1H, H_{Ar}), 7.32−7.22 (m, 1H, H_{Ar}), 7.11−6.98 (m, 2H, H_{Ar}), 6.98−6.85 (m, 1H, H_{Ar}), 6.89−6.74 (m, 2H, H_{Ar}), 6.44 (d, J = 7.6 Hz, 1H, H_{Ar}), 4.51 (br, 1H, N*H*), 3.72 (s, 3H, CH_3), 3.39 (s, 3H, CH_3). $^{13}C\{^{1}H\}$ NMR (101 MHz, $CDCl_3$) δ 156.30, 155.13, 132.76, 132.37, 130.52, 130.38, 122.72, 121.43, 120.91, 120.13, 112.80, 107.17, 106.12, 55.76, 28.00. MS (APCI): *m*/*z* 254.1138 $(M + H)^+$.

Synthesis of (2,6-Diisopropylphenyl)-(4-methyl-6-nitrophenyl)amine (b1). An oven-dried 250 mL Schlenk flask was charged with 4-bromo-3-nitrotoluene (4.32 g, 20 mmol) and 50 mL of toluene. 2,6-Diisopropylaniline (5.32 g, 30 mmol), $Pd_2(dpa)_3$ (0.45 g, 0.5 mmol), *rac*-2,2′-bis(diphenylphosphino)-1,1′-binaphthyl (±BINAP) (0.46 g, 0.75 mmol), and Cs_2CO_3 (3.26 g, 10 mmol) were added to the solution. The reaction mixture was degassed and refilled with nitrogen gas three times and sealed afterward. The flask was heated to 110 °C for 24 h and then cooled to room temperature. The resulting slurry was filtered through a pad of Celite followed by removal of the solvent on a rotatory evaporator, and the final product was purified by chromatography on silica gel with the eluent of *n*-hexane/ethyl acetate (15/1), affording (2,6-diisopropylphenyl)-(2-methyl-6-nitro-phenyl)amine as a yellow powder after the removal of the solvent. Yield: 5.0 g (81%). ^{1}H NMR (400 MHz, $CDCl_3$) δ 9.04 (s, 1H, N*H*), 7.96 (s, 1H, H_{Ar}), 7.33−7.25 (m, 1H, H_{Ar}), 7.21−7.14 (m, 2H, H_{Ar}), 7.02 (d, J = 8.7 Hz, 1H, H_{Ar}), 6.23 (d, J = 8.7 Hz, 1H, H_{Ar}), 2.96 (hept, J = 6.8 Hz, 2H, $CH(CH_3)_2$), 2.20 (s, 3H, CH_3), 1.10 (d, J = 6.8 Hz, 6H, CH_3), 1.04 (d, J = 6.8 Hz, 6H, CH_3). $^{13}C\{^{1}H\}$ NMR (101 MHz, $CDCl_3$) δ 147.33, 144.01, 137.53, 132.70, 131.29, 128.52, 125.96, 125.73, 124.18, 115.49, 28.22, 24.63, 22.98, 19.65. MS (APCI): *m*/*z* 313.1809 $(M + H)^+$.

Compound **b2** was prepared using a similar method as that for **a2**. Yield: 1.4 g (72%). ^{1}H NMR (400 MHz, $CDCl_3$) δ 7.44 (d, J = 7.9 Hz, 1H, H_{Ar}), 7.32−7.24 (m, 2H, H_{Ar}), 7.23−7.17 (m, 1H, H_{Ar}), 6.77−6.70 (m, 1H, H_{Ar}), 6.52 (d, J = 7.9 Hz, 1H, H_{Ar}), 4.51 (br, 2H, NH_2), 2.44 (hept, J = 6.8 Hz, 2H, $CH(CH_3)_2$), 2.36 (s, 3H, CH_3), 1.08 (d, J = 6.8 Hz, 5H, $CH(CH_3)_2$), 0.95 (d, J = 6.8 Hz, 6H, $CH(CH_3)_2$). $^{13}C\{^{1}H\}$ NMR (101 MHz, $CDCl_3$) δ 153.63, 148.57, 142.44, 133.79, 131.33, 130.51, 128.88, 124.78, 121.11, 116.73, 108.00, 28.30, 24.38, 23.88, 21.58. MS (APCI): *m*/*z* 308.2060 $(M + H)^+$.

The ligand **b** was prepared using a similar method as that for ligand **a**. Yield: 0.74 g (94%). ^{1}H NMR (400 MHz, $CDCl_3$) δ 7.56−7.46 (m, 1H, H_{Ar}), 7.36 (d, J = 7.8 Hz, 2H, H_{Ar}), 6.79 (s, 1H, H_{Ar}), 6.70 (d, J = 7.8 Hz, 1H, H_{Ar}), 6.29 (d, J = 7.8 Hz, 1H, H_{Ar}), 4.33 (br, 1H, N*H*), 3.52 (s, 3H, CH_3), 2.67 (hept, J = 6.9 Hz, 2H, $CH(CH_3)_2$), 2.40 (s, 3H, CH_3), 1.18 (d, J = 6.9 Hz, 6H, $CH(CH_3)_2$), 1.05 (d, J = 6.9 Hz, 6H, $CH(CH_3)_2$). $^{13}C\{^{1}H\}$ NMR (101 MHz, $CDCl_3$) δ 155.90, 149.36, 132.66, 130.87, 130.69, 130.25, 128.66, 124.74, 120.77, 107.20, 106.61, 28.45, 28.08, 24.19, 24.09, 21.49. MS (APCI): *m*/*z* 322.2706 $(M + H)^+$.

Synthesis of 1-(2-Methoxyphenyl)-3-methylbenzimidazolin-2-iminato Uranium(IV) (Complex 1) [(Bim$^{2\text{-MeOPh/Me}}$N)UN″$_3$]. A solution of the uranium metallacycle (0.11 g, 1.5 mmol) in 2 mL of toluene was reacted with 1.0 equiv of ligand **a** in 3 mL of toluene. The reaction mixture was stirred at room temperature for 12 h, and after partial removal of the solvent, recrystallization from the concentrated toluene solution afforded the target complex as deep-brown crystals in high yield. Yield: 0.13 g (90%). ^{1}H NMR (300 MHz, C_6D_6) δ 26.36 (d, J = 7.6 Hz, 1H, H_{Ar}), 15.19 (d, J = 7.6 Hz, 1H, H_{Ar}), 12.18 (d, J = 7.1 Hz, 1H, H_{Ar}), 9.22−9.10 (m, 1H, H_{Ar}), 7.13−7.04 (m, 1H, H_{Ar}), 2.06 (s, 1H, H_{Ar}), 0.13 to −0.07 (m, 1H, H_{Ar}), −2.76 to −2.93 (m, 1H, H_{Ar}), −5.02 to −5.91 (t, 3H, CH_3), −6.88 (s, 3H, CH_3), −10.48 to −12.28 (br, 54H, $N(SiMe_3)_2$). $^{13}C\{^{1}H\}$ NMR (75 MHz, C_6D_6) δ 160.28, 136.33, 132.83, 129.87, 128.83, 128.06, 125.19, 116.30, 116.28, 112.18, 108.63, 43.41, 20.94, 6.47. Anal. Calcd for $C_{33}H_{68}N_6OSi_6U$: C, 40.80, H, 7.06, N, 8.65. Found: C, 40.41, H, 6.98, N, 8.61.

Synthesis of 1-(2-Methoxyphenyl)-3-methylbenzimidazolin-2-iminato Thorium(IV) (Complex 2) [(Bim$^{2\text{-MeOPh/Me}}$N)ThN″$_3$]. A

DOI: 10.1021/acs.organomet.7b00432
Organometallics XXXX, XXX, XXX−XXX

solution of the thorium metallacycle (0.11 g, 1.5 mmol) in 2 mL of toluene was reacted with 1.0 equiv of ligand **a** in 3 mL of toluene. The reaction mixture was stirred at room temperature for 12 h, and after partial removal of the solvent, recrystallization from the concentrated toluene solution afforded the target complex as colorless crystals in high yield. Yield: 0.13 g (92%). ^{1}H NMR (300 MHz, C_6D_6) δ 7.30 (d, J = 7.7 Hz, 1H, H_{Ar}), 7.12−7.03 (m, 1H, H_{Ar}), 6.91−6.80 (m, 2H, H_{Ar}), 6.76 (d, J = 7.7 Hz, 1H, H_{Ar}), 6.55−6.47 (m, 2H, H_{Ar}), 6.35 (d, J = 7.7 Hz, 1H, H_{Ar}), 3.30 (s, 3H, CH_3), 3.09 (s, 3H, CH_3), 0.37 (s, 54H, $N(SiMe_3)_2$). $^{13}C\{^1H\}$ NMR (75 MHz, C_6D_6) δ 156.14, 143.63, 131.56, 131.27, 131.13, 129.90, 128.84, 124.41, 120.99, 120.86, 111.61, 108.01, 106.48, 54.33, 28.58, 4.37. Anal. Calcd for $C_{33}H_{68}N_6OSi_6Th$: C, 41.05, H, 7.10, N, 8.70. Found: C, 40.62, H, 7.04, N, 8.68.

Synthesis of 1-(2,6-Diisopropylphenyl)-3,5-dimethyl-1,3-dihydro-benzimidazolin-2-imine Uranium(IV) (Complex 3) [(Bim$_{5\text{-Me}}^{Dipp/Me}$N)UN″$_3$]. Complex **3** was prepared using a similar method as for the synthesis of **1** and isolated as deep-brown crystals. Yield: 0.15 g (94%). ^{1}H NMR (300 MHz, C_6D_6) δ 97.04 (s, 2H, $CH(CH_3)_2$), 25.95 (s, 1H, H_{Ar}), 14.32 (s, 9H, $CH(CH_3)_2$ and CH_3), 12.00 (d, J = 6.6 Hz, 1H, H_{Ar}), 9.41 (d, J = 6.6 Hz, 1H, H_{Ar}), 8.35 (s, 3H, CH_3), −0.17 (s, 6H, $CH(CH_3)_2$), −0.54 to −0.73 (m, 1H, H_{Ar}), −2.75 (b, 2H, H_{Ar}), −12.41 (b, 42H, $N(Si(CH_3)_3)_2$), −20.27 (s, 12H, $N(Si(CH_3)_3)_2$). $^{13}C\{^1H\}$ NMR (75 MHz, C_6D_6) δ 169.82, 157.27, 141.96, 131.35, 129.21, 126.59, 126.53, 120.08, 118.61, 116.76, 111.40, 34.12, 28.76, 23.01, 18.53, 8.43. Anal. Calcd for $C_{39}H_{80}N_6Si_6U$: C, 45.06, H, 7.76, N, 8.08, Found: C, 45.20, H, 7.86; N, 8.00.

Synthesis of 1-(2,6-Diisopropylphenyl)-3,5-dimethyl-1,3-dihydro-benzimidazolin-2-imine Thorium(IV) (Complex 4) [(Bim$_{5\text{-Me}}^{Dipp/Me}$N) ThN″$_3$]. Complex **4** was prepared using a similar method as for the synthesis of **2** and isolated as colorless crystals. Yield: 0.14 g 92%. ^{1}H NMR (300 MHz, C_6D_6) δ 7.34−7.04 (m, 3H, H_{Ar}), 6.52 (d, J = 7.8 Hz, 1H, H_{Ar}), 6.36 (s, 1H, H_{Ar}), 6.12 (d, J = 7.8 Hz, 1H, H_{Ar}), 3.38 (s, 3H, CH_3), 2.88 (hept, J = 6.7 Hz, 2H, $CH(CH_3)_2$), 2.16 (s, 3H, CH_3), 1.26 (d, J = 6.7 Hz, 6H, $CH(CH_3)_2$), 0.87 (d, J = 6.7 Hz, 6H, $CH(CH_3)_2$), 0.52−0.14 (m, 54H, $N(Si(CH_3)_3)_2$). $^{13}C\{^1H\}$ NMR (75 MHz, C_6D_6) δ 148.02, 144.42, 131.58, 131.16, 130.45, 129.97, 129.35, 128.84, 125.20, 124.34, 121.18, 109.11, 107.35, 29.33, 28.20, 25.16, 23.75, 21.02, 4.74, 3.53. Anal. Calcd for $C_{39}H_{80}N_6Si_6U$: C, 45.32, H, 7.80, N, 8.13. Found: C, 45.26, H, 7.76; N, 8.09.

General Procedure for the Catalytic Addition of Alcohols into Carbodiimides. For Th(IV) complexes, a sealable J. Young NMR tube was loaded with approximately 2 mol % of the desired catalyst from a stock solution in C_6D_6 inside the glovebox, followed by the addition of carbodiimide (0.35 mmol, 50 equiv) and alcohol (0.35 mmol, 50 equiv). The reaction was immediately diluted to 500 μL with C_6D_6. Samples were taken out of the glovebox, and the reaction progress was monitored by ^{1}H NMR spectroscopy. The crude mixtures were analyzed using ^{1}H and ^{13}C NMR spectroscopy and mass spectrometry; the values were compared to previously published data.[69]

For U(IV) complexes, due to their paramagnetic properties, a different method was applied. A 10 mL vial was loaded with 2 mol % of the desired catalyst from a stock solution in C_6D_6, followed by the addition of carbodiimide (0.35 mmol, 50 equiv) and alcohol (0.35 mmol, 50 equiv). The reaction was immediately diluted to 500 μL with C_6D_6. A 40 μL sample of the reaction mixture was taken every hour and diluted with C_6D_6. ^{1}H NMR spectroscopy was performed on the sample immediately to monitor the process.

The NMR spectra for the catalytic insertion of MeOH, EtOH, ^{i}PrOH, ^{t}BuOH, PhOH, 2,6-Me$_2$PhOH, 2,4-^{t}BuPhOH, $HO(CH_2)_3OH$, and $N(CH_2CH_2OH)_3$ into DTC were compared with previous reports.[69]

Preparative Scale-up Reaction. In the glovebox, a solution of methanol (0.2 mL, 5 mmol) in toluene (1 mL) was added to a solution of complex **2** (96 mg, 0.1 mmol) in toluene (1 mL) in a Schlenk tube. DTC (1.11 g, 5 mmol) was then added to the above reaction mixture. The Schlenk tube was taken outside the glovebox, and the mixture was stirred at room temperature for 3 h. After the solvent was removed under reduced pressure, the residue was extracted with toluene and filtered to give a clean solution. After removal of part of the solvent, subsequent recrystallization from toluene gave the final isourea products in 95% (1.2 g) yield. This method is also general for isolating other insertion products.

Insertion of Benzyl Alcohol (BnOH) into DTC. The insertion of benzyl alcohol into DTC was carried out following the general procedure described above. ^{1}H NMR (300 MHz, C_6D_6) δ 7.55−7.31 (m, 2H, H_{Ar}), 7.31−7.06 (m, 7H, H_{Ar}), 7.01−6.81 (m, 4H, H_{Ar}), 6.03 (s, 1H, NH), 5.55 (s, 2H, CH_2), 2.26 (s, 3H, CH_3), 2.11 (s, 3H, CH_3). $^{13}C\{^1H\}$ NMR (75 MHz, C_6D_6) δ 149.77, 145.96, 137.12, 136.29, 132.25, 131.90, 130.48, 129.34, 128.41, 128.10, 122.69, 120.84, 68.34, 20.75, 20.44. MS (APCI): 331.1897 $(M + H)^+$.

Insertion of 2-Pyridinemethanol (Py-2-CH$_2$OH) into DTC. The insertion of 2-pyridinemethanol into DTC was carried out following the general procedure described above. ^{1}H NMR (300 MHz, C_6D_6) δ 8.61−8.34 (m, 1H, H_{Ar}), 7.45−6.83 (m, 10H, H_{Ar}), 6.75−6.58 (m, 1H, H_{Ar}), 6.25 (s, 1H, NH), 5.79 (s, 2H, CH_2), 2.23 (s, 3H, CH_3), 2.14 (s, 3H, CH_3). $^{13}C\{^1H\}$ NMR (50 MHz, C_6D_6) δ 157.32, 149.56, 149.25, 145.79, 132.37, 131.82, 130.33, 129.35, 128.10, 122.64, 122.03, 121.17, 121.10, 69.00, 20.58, 20.49. MS (APCI): 331.2009 $(M)^+$.

Insertion of 2-Thiophenemethanol (Thio-2-CH$_2$OH) into DTC. The insertion of 2-thiophenemethanol into DTC was carried out following the general procedure described above. ^{1}H NMR (300 MHz, C_6D_6) δ 7.38−7.06 (m, 5H, H_{Ar}), 7.04−6.65 (m, 7H, H_{Ar}), 5.96 (br, 1H, NH), 5.60 (s, 2H, CH_2), 2.27 (s, 3H, CH_3), 2.10 (s, 3H, CH_3). $^{13}C\{^1H\}$ NMR (75 MHz, C_6D_6) δ 149.43, 145.76, 139.12, 136.11, 132.32, 132.00, 130.47, 130.18, 129.31, 126.80, 126.30, 124.15, 122.72, 120.91, 62.58, 20.64, 20.41. MS (APCI): 337.1412 $(M + H)^+$.

Insertion of 2-Furanmethanol (Furan-2-CH$_2$OH) into DTC. The insertion of 2-furanmethanol into DTC was carried out following the general procedure described above. ^{1}H NMR (300 MHz, C_6D_6) δ 7.30−7.20 (m, 1H, H_{Ar}), 7.17−7.01 (m, 4H, H_{Ar}), 6.97−6.77 (m, 4H, H_{Ar}), 6.37−6.24 (m, 1H, H_{Ar}), 6.15−6.02 (m, 1H, H_{Ar}), 5.95 (br, 1H, NH), 5.49 (s, 2H, CH_2), 2.26 (s, 3H, CH_3), 2.09 (s, 3H, CH_3). $^{13}C\{^1H\}$ NMR (75 MHz, C_6D_6) δ 150.67, 149.46, 145.81, 142.76, 136.20, 132.19, 131.93, 130.45, 129.32, 122.67, 120.61, 110.47, 99.88, 60.14, 20.66, 20.13. MS (APCI): 321.1659 $(M + H)^+$.

Insertion of Cyclohexanol (CyOH) into DTC. The insertion of cyclohexanol into DTC was carried out following the general procedure described above. ^{1}H NMR (300 MHz, C_6D_6) δ 7.25−6.69 (m, 8H, H_{Ar}), 6.01 (br, 1H, NH), 5.70−5.30 (m, 1H, CH), 2.44−1.86 (m, 8H, CH_3 and CH_2), 1.83−1.53 (m, 4H, CH_2), 1.33 (m, 4H, CH_2). $^{13}C\{^1H\}$ NMR (75 MHz, C_6D_6) δ 149.18, 146.31, 136.74, 131.90, 131.60, 130.49, 129.26, 122.70, 120.57, 74.09, 31.66, 25.65, 23.67, 20.65, 20.42. MS (APCI): 323.2176 $(M + H)^+$.

Insertion of Diphenylmethanol (Ph$_2$CHOH) into DTC. The insertion of diphenylmethanol into DTC was carried out following the general procedure described above. ^{1}H NMR (300 MHz, C_6D_6) δ 7.75 (s, 1H, CH), 7.63−7.43 (m, 4H, H_{Ar}), 7.31−6.77 (m, 14H, H_{Ar}), 5.98 (br, 1H, NH), 2.22−2.14 (s, 6H, CH_3). $^{13}C\{^1H\}$ NMR (75 MHz, C_6D_6) δ 148.96, 145.73, 141.51, 136.28, 136.22, 132.57, 131.89, 130.38, 129.35, 124.15, 122.59, 121.39, 79.08, 20.64, 20.54. MS (APCI): 407.2197 $(M + H)^+$.

Insertion of 1-adamantanol into DTC. The insertion of 1-adamantanol into DTC was carried out following the general procedure described above. ^{1}H NMR (300 MHz, C_6D_6) δ 7.26−6.71 (m, 8H, H_{Ar}), 5.93 (br, 1H, NH), 2.46 (br, 6H, CH_2), 2.36−1.98 (m, 9H, CH_3 and CH), 1.78−1.41 (m, 6H, CH_2). $^{13}C\{^1H\}$ NMR (75 MHz, C_6D_6) δ 147.92, 146.20, 131.55, 131.41, 130.16, 129.26, 124.12, 122.60, 120.44, 81.01, 41.80, 36.33, 31.17, 20.63, 20.56. MS (APCI): 375.2452$(M + H)^+$.

Insertion of Methanol into 1,3-Dimesitylcarbodiimide ((Mes)NCN(Mes)). The insertion of MeOH into (Mes)NCN(Mes) was carried out following the general procedure described above. ^{1}H NMR (300 MHz, C_6D_6) δ 6.90 (s, 2H, H_{Ar}), 6.58 (s, 2H H_{Ar}), 4.44 (s, 1H, NH), 3.60 (s, 3H, CH_3), 2.30 (s, 6H, CH_3), 2.24 (s, 3H, CH_3), 2.04 (s, 3H, CH_3), 1.98 (s, 6H, CH_3). $^{13}C\{^1H\}$ NMR (75 MHz, C_6D_6) δ 149.37, 142.89, 135.62, 132.97, 132.09, 130.85, 129.28, 129.05, 128.85, 128.38, 53.05, 20.47, 20.40, 18.11, 17.89. MS (APCI): 311.2160 $(M + H)^+$.

DOI: 10.1021/acs.organomet.7b00432
Organometallics XXXX, XXX, XXX−XXX

Insertion of Methanol into 1,3-Di-*p*-chlorophenylcarbodiimide ((4-ClPh)NCN(4-ClPh)). The insertion of MeOH into (4-ClPh)NCN(4-ClPh) was carried out following the general procedure described above. ^{1}H NMR (300 MHz, C_6D_6) δ 7.07 (s, 2H, H_{Ar}), 6.92 (s, 2H, H_{Ar}), 6.62 (s, 2H, H_{Ar}), 6.40 (s, 2H, H_{Ar}), 5.45 (s, 1H, N*H*), 3.55 (s, 3H, C*H*$_3$).^{13}C{^{1}H} NMR (75 MHz, C_6D_6) δ 149.57, 129.59, 128.54, 123.72, 121.72, 53.42. MS (APCI): 295.0438 $(M + H)^+$.

Insertion of Methanol into 1,3-Di-*p*-methoxylphenylcarbodiimide ((4-MeOPh)NCN(4-MeOPh)). The insertion of MeOH into (4-MeOPh)NCN(4-MeOPh) was carried out following the general procedure described above. ^{1}H NMR (300 MHz, C_6D_6) δ 7.08−6.85 (m, 2H, H_{Ar}), 6.85−6.66 (m, 4H, H_{Ar}), 6.66−6.50 (m, 2H, H_{Ar}), 5.78 (s, 1H, N*H*), 3.70 (s, 3H, OC*H*$_3$), 3.32 (s, 3H, C*H*$_3$), 3.24 (s, 3H, C*H*$_3$). ^{13}C{^{1}H} NMR (75 MHz, C_6D_6) δ 156.19, 155.60, 150.92, 141.40, 131.58, 124.88, 123.07, 114.97, 113.77, 54.54, 53.15. MS (APCI): 287.1434 $(M + H)^+$.

Insertion of 1,4-Benzenedimethanol into DTC. The insertion of 1,4-benzenedimethanol into DTC was carried out following the general procedure described above, except at 50 °C due to the poor solubilities of substrates in C_6D_6. ^{1}H NMR (300 MHz, C_6D_6) δ 7.21 (s, 4H, H_{Ar}), 7.05−6.89 (m, 8H, H_{Ar}), 6.81−6.64 (m, 8H, H_{Ar}), 5.87 (s, 8H, N*H*), 5.37 (s, 4H, C*H*$_2$), 2.12 (s, 6H, C*H*$_3$), 1.97 (s, 6H, C*H*$_3$). ^{13}C{^{1}H} NMR (75 MHz, C_6D_6) δ 149.50, 145.72, 136.33, 136.07, 132.03, 131.69, 130.24, 129.11, 127.95, 122.46, 120.60, 67.85, 20.40, 20.21. MS (APCI): *m*/*z* 583.02 $(M + H)^+$.

Insertion of 1,4-Butynediol into DTC. The insertion of 1,4-butynediol into DTC was carried out following the general procedure described above, except at 50 °C due to the poor solubilities of substrates in C_6D_6. ^{1}H NMR (300 MHz, C_6D_6) δ 7.25−6.61 (m, 16H, H_{Ar}), 5.94 (br, 2H, N*H*), 5.05 (br, 4H, C*H*$_2$), 2.11 (br, 12H, C*H*$_3$). ^{13}C{^{1}H} NMR (75 MHz, C_6D_6) δ148.71, 145.20, 135.78, 132.17, 131.71, 129.16, 123.78, 122.36, 120.73, 81.54, 53.99, 20.47, 20.30. MS (APCI): 531.2822 $(M + H)^+$.

Insertion of 1,3-Butanediol into DTC. The insertion of 1,3-butanediol into DTC was carried out following the general procedure described above. For the monoisourea compounds **8a** and **8b**, molar ratio of 1/1 between 1,3-butanediol and DTC was applied, and the product ratio between **8a** and **8b** was calculated from CH assignment; to this reaction mixture was added another equivalent of DTC affording the final diisourea products. ^{1}H NMR (300 MHz, C_6D_6) δ 7.06−6.86 (m, 8H, H_{Ar}), 6.91−6.67 (m, 8H, H_{Ar}), 5.82 (d, 2H, N*H*), 5.69−5.55 (m, 1H, C*H*), 4.55 (t, J = 5.9 Hz, 2H, C*H*$_2$), 2.08 (br, 6H, C*H*$_3$), 1.97 (br, 6H, C*H*$_3$), 1.88−1.70 (m, 2H, C*H*$_2$), 1.23 (d, J = 6.0 Hz, 1H, C*H*$_2$). ^{13}C{^{1}H} NMR (75 MHz, C_6D_6) δ 149.72, 149.26, 145.99, 136.28, 136.18, 136.07, 134.79, 131.99, 131.46, 131.41, 130.15, 129.92, 129.16, 129.10, 123.88, 122.51, 120.85, 69.88, 63.24, 35.14, 20.36, 20.18, 19.68. MS (APCI: 557.2941 $(M + Na)^+$.

Stoichiometric Reactions between Complex 4 and Three Equivalents of 2,4-^{t}Bu$_2$PhOH To Prepare Active Species CatA. A J. Young NMR tube was loaded with 20.0 mg (19.3 mmol) of thorium complex **4** [$(Bim_{5\text{-}Me}{}^{Dipp/Me}N)ThN''_3$], 3.0 equiv of 2,4-^{t}Bu$_2$PhOH (12.0 mg, 58 mmol), and 500 μL of C_6D_6. Then the tube was taken out of the glovebox and monitored by ^{1}H NMR spectroscopy. The release of $HN(SiMe_3)_2$ was immediately observed, as evidenced from the appearance of the characteristic peak of the methyl group at δ = 0.05 ppm, and the reaction can be completed in 1 h, affording the [$(Bim_{5\text{-}Me}{}^{Dipp/Me}N)Th(O\text{-}2,4\text{-}{}^tBu_2Ph)_3$] intermediate (Figure S44 and S45). [$(Bim_{5\text{-}Me}{}^{Dipp/Me}N)Th(O\text{-}2,4\text{-}{}^tBu_2Ph)_3$]: ^{1}H NMR (300 MHz, C_6D_6) δ 7.50−7.35 (m, 4H, H_{Ar}), 7.03−6.85 (m, 9H, H_{Ar}), 6.62−6.39 (m, 2H, H_{Ar}), 3.52 (s, 3H, CH_3), 2.62 (s, 2H, CH), 1.56 (s, 27H, C(C*H*$_3$)$_3$), 1.49−1.38 (m, 12H, CH(C*H*$_3$)$_2$), 1.28 (s, 30H,C(C*H*$_3$)$_3$ and CH_3), 1.03−0.82 (m, 12H, CH(C*H*$_3$)$_2$), 0.05 (s, 54H, Si(C*H*$_3$)$_2$). ^{13}C NMR (75 MHz, C_6D_6) δ 162.24, 157.74, 148.51, 139.47, 136.06, 125.27, 124.96, 124.64, 123.77, 123.35, 122.89, 121.61, 34.70, 33.83, 31.58, 30.57, 30.35, 28.38, 22.67, 15.78.

Kinetic Studies of 2,4-^{t}Bu$_2$PhOH insertion into DTC Using Complex 2. All the kinetic experiments were performed following a similar method. In a J. Young NMR tube, 2 mol % precatalyst **2**, DTC (0.35 mmol, 50 equiv), 2,4-^{t}Bu$_2$PhOH (0.35 mmol, 50 equiv), and C_6D_6 were mixed in the glovebox, and then the tube was sealed. The tube was taken out of the glovebox and frozen in an ice bath until the ^{1}H NMR experiment began. All the experiments were done by changing one substrate or catalyst while keeping the other reagents constant, and the progress of the reaction was initially monitored every 2 min and then in longer intervals up to 1.5 h. The product concentrations were measured by the area ratio of the *tert*-butyl group at 1.11 and 1.23 ppm, which were assigned to the starting material and reaction product, respectively. Reaction rates were determined by least-squares fit of the initial product concentration versus time, and the plots of the initial reaction rates against precatalyst **2**, DTC, and 2,4-^{t}Bu$_2$PhOH are shown in Figures 4−6.

Activation parameters including enthalpy ($\Delta H^{\ddagger}$), entropy ($\Delta S^{\ddagger}$), and activation energy (E_a) were calculated from the kinetic data using Eyring and Arrhenius plots. In a typical sample, the J. Young tube was loaded with the desired amount of catalyst **2**, DTC, 2,4-di-*tert*-butylphenol, and solvent and then was sealed and frozen. Then the sample was inserted into a Bruker Avance 300 spectrometer, which had been previously set to the desired temperature. The progress was initially monitored every minute and then in longer intervals up to one and a half hours. Reaction rates were determined by least-squares fit of the initial product concentration versus time, and Eyring and Arrhenius plots are shown in Figure 7. Enthalpy ($\Delta H^{\ddagger}$), entropy ($\Delta S^{\ddagger}$), and activation energy (E_a) were calculated from the slope and intercept of the least-squares fit.

Deuterium labeling studies using 2,4-^{t}Bu$_2$PhOD and DTC indicated that the insertion of DTC into **CatA** is the turnover limiting step during the catalytic cycle, and the remaining steps of the cycle are rapid, so the following rate equation can be obtained based on the assumption of a steady-state:

$$\frac{\partial p}{\partial t} = k_1[\mathbf{CatA}][\mathrm{DTC}]$$

In the beginning step, formation of active **CatA**, that is, alcoholysis of [$(Bim^{R_1/R_2}N)AnN''_3$], is rapid and irreversible; however, the equilibrium of alcohol coordination/decoordination to the actinide center must be considered (this step has been verified in similar benzimidazolin-2-iminato actinide systems in our previous report),[69] giving the following expression:

$$K_{eq} = \frac{[\text{sat } \mathbf{CatA}]}{[\mathrm{R'OH}][\mathbf{CatA}]}$$

From the reaction cycle, it can be found that the sum of active catalysts (**CatA**) and alcohol-saturated complex (sat **CatA**) is the total amount of catalyst loading [An] used in the reaction: [**CatA**] + [sat **CatA**] = [An]. After substitution of [**CatA**] from the equilibrium expression into the rate equation, the following kinetic rate law is obtained:

$$\frac{\partial p}{\partial t} = k_1\frac{[\mathrm{An}][\mathrm{DTC}]}{(1 + K_{eq}[\mathrm{R'OH}])}$$

From this equation, inverse-first order behavior can be concluded if $K_{eq}[\mathrm{R'OH}] \gg 1$.

Deuterium Labeling Studies. All the deuterium labeling experiments were done with a similar method. In a J. Young NMR tube, 2 mol % precatalyst **2**, DTC (0.35 mmol, 50 equiv), and 2,4-^{t}Bu$_2$PhOH (or 2,4-^{t}Bu$_2$PhOD) (0.35 mmol, 50 equiv) were added in the glovebox and then diluted to 0.5 mL using C_6D_6. The tube was sealed and taken out of the glovebox and cooled in an ice bath until the ^{1}H NMR experiment began at 25 °C. The progress was initially monitored every minute and then in longer intervals up to one and a half hours. The product concentration was measured by the integrated area ratio of *tert*-butyl group at 1.11 and 1.23 ppm, which were assigned to the starting material and reaction product, respectively. Reaction rates were determined by least-squares fit of the initial product concentration versus time. The KIE value was calculated from the ratio of the two slopes.

DOI: 10.1021/acs.organomet.7b00432
Organometallics XXXX, XXX, XXX−XXX

■ ASSOCIATED CONTENT

Supporting Information

The Supporting Information is available free of charge on the ACS Publications website at DOI: 10.1021/acs.organomet.7b00432.

Crystallographic data for complexes **1**−**4** and ^{1}H NMR and ^{13}C NMR for **CatA**, ligands, complexes, and isourea products (PDF)

Accession Codes

CCDC 1544404−1544407 contain the supplementary crystallographic data for this paper. These data can be obtained free of charge via www.ccdc.cam.ac.uk/data_request/cif, or by emailing data_request@ccdc.cam.ac.uk, or by contacting The Cambridge Crystallographic Data Centre, 12 Union Road, Cambridge CB2 1EZ, UK; fax: +44 1223 336033.

■ AUTHOR INFORMATION

Corresponding Authors

*E-mail: chmoris@tx.technion.ac.il. Phone: +972-4-8292680 (M.S.E.).
*E-mail: m.tamm@tu-bs.de (M.T.).

ORCID

Heng Liu: 0000-0002-6035-3428
Matthias Tamm: 0000-0002-5364-0357
Moris S. Eisen: 0000-0001-8915-0256

Author Contributions

The manuscript was written through contributions of all authors. All authors have given approval to the final version of the manuscript

Notes

The authors declare no competing financial interest.

■ ACKNOWLEDGMENTS

This work was supported by the German Israel Foundation (GIF) under Contract I-1264-302.5/2014 and by the PAZY Foundation Fund (2015) administered by the Israel Atomic Energy Commission, and H.L. was supported by the Technion-Guangdong Fellowship.

■ REFERENCES

(1) Shigehisa, H.; Hayashi, M.; Ohkawa, H.; Suzuki, T.; Okayasu, H.; Mukai, M.; Yamazaki, A.; Kawai, R.; Kikuchi, H.; Satoh, Y.; Fukuyama, A.; Hiroya, K. *J. Am. Chem. Soc.* **2016**, *138*, 10597−10604.
(2) Shepard, S. M.; Diaconescu, P. L. *Organometallics* **2016**, *35*, 2446−2453.
(3) Liu, Z.; Breit, B. *Angew. Chem. Int. Ed.* **2016**, *55*, 8440−8443.
(4) Martínez, J.; Otero, A.; Lara-Sánchez, A.; Castro-Osma, J. A.; Fernández-Baeza, J.; Sánchez-Barba, L. F.; Rodríguez, A. M. *Organometallics* **2016**, *35*, 1802−1812.
(5) Brooner, R. E. M.; Brown, T. J.; Chee, M. A.; Widenhoefer, R. A. *Organometallics* **2016**, *35*, 2014−2021.
(6) Wathier, M.; Love, J. A. *Eur. J. Inorg. Chem.* **2016**, *2016*, 2391−2402.
(7) Notar Francesco, I.; Cacciuttolo, B.; Pascu, O.; Aymonier, C.; Pucheault, M.; Antoniotti, S. *RSC Adv.* **2016**, *6*, 19807−19818.
(8) Rodriguez-Ruiz, V.; Carlino, R.; Bezzenine-Lafollee, S.; Gil, R.; Prim, D.; Schulz, E.; Hannedouche, J. *Dalton Trans.* **2015**, *44*, 12029−12059.
(9) Lam, R. H.; Walker, D. B.; Tucker, M. H.; Gatus, M. R. D.; Bhadbhade, M.; Messerle, B. A. *Organometallics* **2015**, *34*, 4312−4317.
(10) Veenboer, R. M. P.; Dupuy, S.; Nolan, S. P. *ACS Catal.* **2015**, *5*, 1330−1334.
(11) Choy, S. W. S.; Page, M. J.; Bhadbhade, M.; Messerle, B. A. *Organometallics* **2013**, *32*, 4726−4729.
(12) Shigehisa, H.; Aoki, T.; Yamaguchi, S.; Shimizu, N.; Hiroya, K. *J. Am. Chem. Soc.* **2013**, *135*, 10306−10309.
(13) Bigot, S.; El Alami, M. S. I.; Mifleur, A.; Castanet, Y.; Suisse, I.; Mortreux, A.; Sauthier, M. *Chem. - Eur. J.* **2013**, *19*, 9785−9788.
(14) Weiss, C. J.; Marks, T. J. *Dalton Trans.* **2010**, *39*, 6576−6588.
(15) Seo, S.; Yu, X.; Marks, T. J. *J. Am. Chem. Soc.* **2009**, *131*, 263−276.
(16) Yu, X.; Seo, S.; Marks, T. J. *J. Am. Chem. Soc.* **2007**, *129*, 7244−7245.
(17) Däbritz, E. *Angew. Chem., Int. Ed. Engl.* **1966**, *5*, 470−477.
(18) Batrice, R. J.; Eisen, M. S. *Chem. Sci.* **2016**, *7*, 939−944.
(19) Zhang, W.; Xu, L.; Xi, Z. *Chem. Commun.* **2015**, *51*, 254−265.
(20) Xue, M.; Zheng, Y.; Hong, Y.; Yao, Y.; Xu, F.; Zhang, Y.; Shen, Q. *Dalton Trans.* **2015**, *44*, 20075−20086.
(21) Behrle, A. C.; Schmidt, J. A. R. *Organometallics* **2013**, *32*, 1141−1149.
(22) Zhou, S.; Wang, S.; Yang, G.; Li, Q.; Zhang, L.; Yao, Z.; Zhou, Z.; Song, H.-b. *Organometallics* **2007**, *26*, 3755−3761.
(23) Zhang, W.; Nishiura, M.; Hou, Z. *Chem. Commun.* **2006**, 3812−3814.
(24) Mathias, L. J. *Synthesis* **1979**, 561−576.
(25) Haskel, A.; Straub, T.; Eisen, M. S. *Organometallics* **1996**, *15*, 3773−3775.
(26) Straub, T.; Haskel, A.; Neyroud, T. G.; Kapon, M.; Botoshansky, M.; Eisen, M. S. *Organometallics* **2001**, *20*, 5017−5035.
(27) Stubbert, B. D.; Stern, C. L.; Marks, T. J. *Organometallics* **2003**, *22*, 4836−4838.
(28) Stubbert, B. D.; Marks, T. J. *J. Am. Chem. Soc.* **2007**, *129*, 6149−6167.
(29) Broderick, E. M.; Gutzwiller, N. P.; Diaconescu, P. L. *Organometallics* **2010**, *29*, 3242−3251.
(30) Hayes, C. E.; Platel, R. H.; Schafer, L. L.; Leznoff, D. B. *Organometallics* **2012**, *31*, 6732−6740.
(31) Dash, A. K.; Wang, J. X.; Berthet, J. C.; Ephritikhine, M.; Eisen, M. S. *J. Organomet. Chem.* **2000**, *604*, 83−98.
(32) Karmel, I. S. R.; Tamm, M.; Eisen, M. S. *Angew. Chem. Int. Ed.* **2015**, *54*, 12422−12425.
(33) Haskel, A.; Straub, T.; Dash, A. K.; Eisen, M. S. *J. Am. Chem. Soc.* **1999**, *121*, 3014−3024.
(34) Haskel, A.; Wang, J. Q.; Straub, T.; Neyroud, T. G.; Eisen, M. S. *J. Am. Chem. Soc.* **1999**, *121*, 3025−3034.
(35) Wang, J. Q.; Dash, A. K.; Berthet, J. C.; Ephritikhine, M.; Eisen, M. S. *Organometallics* **1999**, *18*, 2407−2409.
(36) Wang, J. X.; Dash, A. K.; Kapon, M.; Berthet, J. C.; Ephritikhine, M.; Eisen, M. S. *Chem. - Eur. J.* **2002**, *8*, 5384−5396.
(37) Kosog, B.; Kefalidis, C. E.; Heinemann, F. W.; Maron, L.; Meyer, K. *J. Am. Chem. Soc.* **2012**, *134*, 12792−12797.
(38) Hayes, C. E.; Leznoff, D. B. *Organometallics* **2010**, *29*, 767−774.
(39) Domeshek, E.; Batrice, R. J.; Aharonovich, S.; Tumanskii, B.; Botoshansky, M.; Eisen, M. S. *Dalton Trans.* **2013**, *42*, 9069−9078.
(40) Mansell, S. M.; Bonnet, F.; Visseaux, M.; Arnold, P. L. *Dalton Trans.* **2013**, *42*, 9033−9039.
(41) Lam, O. P.; Franke, S. M.; Heinemann, F. W.; Meyer, K. *J. Am. Chem. Soc.* **2012**, *134*, 16877−16881.
(42) Schmidt, A.-C.; Nizovtsev, A. V.; Scheurer, A.; Heinemann, F. W.; Meyer, K. *Chem. Commun.* **2012**, *48*, 8634−8636.
(43) Mansell, S. M.; Farnaby, J. H.; Germeroth, A. I.; Arnold, P. L. *Organometallics* **2013**, *32*, 4214−4222.
(44) Mougel, V.; Camp, C.; Pécaut, J.; Copéret, C.; Maron, L.; Kefalidis, C. E.; Mazzanti, M. *Angew. Chem., Int. Ed.* **2012**, *51*, 12280−12284.
(45) Arnold, P. L.; Mansell, S. M.; Maron, L.; McKay, D. *Nat. Chem.* **2012**, *4*, 668−674.
(46) Arnold, P. L.; Turner, Z. R.; Bellabarba, R. M.; Tooze, R. P. *Chem. Sci.* **2011**, *2*, 77−79.
(47) Matson, E. M.; Forrest, W. P.; Fanwick, P. E.; Bart, S. C. *J. Am. Chem. Soc.* **2011**, *133*, 4948−4954.

DOI: 10.1021/acs.organomet.7b00432
Organometallics XXXX, XXX, XXX−XXX

(48) Mansell, S. M.; Kaltsoyannis, N.; Arnold, P. L. *J. Am. Chem. Soc.* **2011**, *133*, 9036−9051.
(49) Lin, Z.; Marks, T. J. *J. Am. Chem. Soc.* **1987**, *109*, 7979−7985.
(50) Arnold, P. L.; Turner, Z. R. *Nat. Rev. Chem.* **2017**, *1*, 0002.
(51) Fox, A. R.; Bart, S. C.; Meyer, K.; Cummins, C. C. *Nature* **2008**, *455*, 341−349.
(52) Karmel, I. S.; Batrice, R. J.; Eisen, M. S. *Inorganics* **2015**, *3*, 392−428.
(53) Berthet, J. C.; Ephritikhine, M. *Coord. Chem. Rev.* **1998**, *178*−*180*, 83−116.
(54) Andrea, T.; Barnea, E.; Eisen, M. S. *J. Am. Chem. Soc.* **2008**, *130*, 2454−2455.
(55) Karmel, I. S. R.; Fridman, N.; Tamm, M.; Eisen, M. S. *Organometallics* **2015**, *34*, 2933−2942.
(56) Karmel, I. S. R.; Botoshansky, M.; Tamm, M.; Eisen, M. S. *Inorg. Chem.* **2014**, *53*, 694−696.
(57) Karmel, I. S. R.; Fridman, N.; Tamm, M.; Eisen, M. S. *J. Am. Chem. Soc.* **2014**, *136*, 17180−17192.
(58) Wobser, S. D.; Marks, T. J. *Organometallics* **2013**, *32*, 2517−2528.
(59) Barnea, E.; Moradove, D.; Berthet, J. C.; Ephritikhine, M.; Eisen, M. S. *Organometallics* **2006**, *25*, 320−322.
(60) Rabinovich, E.; Aharonovich, S.; Botoshansky, M.; Eisen, M. S. *Dalton Trans.* **2010**, *39*, 6667−6676.
(61) Karmel, I. S. R.; Fridman, N.; Eisen, M. S. *Organometallics* **2015**, *34*, 636−643.
(62) Karmel, I. S. R.; Khononov, M.; Tamm, M.; Eisen, M. S. *Catal. Sci. Technol.* **2015**, *5*, 5110.
(63) Walshe, A.; Fang, J.; Maron, L.; Baker, R. J. *Inorg. Chem.* **2013**, *52*, 9077−9086.
(64) Baker, R. J.; Walshe, A. *Chem. Commun.* **2012**, *48*, 985−987.
(65) Weast, R. C.; Astle, M. J.; Beyer, W. H. *CRC Handbook of Chemistry and Physics*. CRC Press: Boca Raton, FL, 1988; Vol. *69*.
(66) Batrice, R. J.; Kefalidis, C. E.; Maron, L.; Eisen, M. S. *J. Am. Chem. Soc.* **2016**, *138*, 2114−2117.
(67) Van der Sluys, W. G.; Sattelberger, A. P. *Chem. Rev.* **1990**, *90*, 1027−1040.
(68) Berg, J. M.; Clark, D. L.; Huffman, J. C.; Morris, D. E.; Sattelberger, A. P.; Streib, W. E.; Van der Sluys, W. G.; Watkin, J. G. *J. Am. Chem. Soc.* **1992**, *114*, 10811−10821.
(69) Liu, H.; Khononov, M.; Fridman, N.; Tamm, M.; Eisen, M. S. *Inorg. Chem.* **2017**, *56*, 3153−3157.
(70) Wu, X.; Tamm, M. *Coord. Chem. Rev.* **2014**, *260*, 116−138.
(71) Cone angle was defined as the solid angle formed with the metal at the vertex and the hydrogen atoms at the perimeter of the cone formed by the coordinating ligands. Please see reference: Tolman, C. A. *Chem. Rev.* **1977**, *77*, 313−348.
(72) Dudnik, A. S.; Weidner, V. L.; Motta, A.; Delferro, M.; Marks, T. J. *Nat. Chem.* **2014**, *6*, 1100−1107.
(73) Dormond, A.; El Bouadili, A.; Aaliti, A.; Moise, C. *J. Organomet. Chem.* **1985**, *288*, C1−C5.
(74) Kurahashi, T.; Kikuchi, A.; Shiro, Y.; Hada, M.; Fujii, H. *Inorg. Chem.* **2010**, *49*, 6664−6672.
(75) Peddarao, T.; Baishya, A.; Barman, M. K.; Kumar, A.; Nembenna, S. *New J. Chem.* **2016**, *40*, 7627−7636.
(76) Ali, A. R.; Ghosh, H.; Patel, B. K. *Tetrahedron Lett.* **2010**, *51*, 1019−1021.
(77) *Kappa CCD Server Software*; Nonius BV: Delft, The Netherlands, 1997.
(78) Otwinowski, Z.; Minor, W. *Methods Enzymol.* **1997**, *276*, 307−326.
(79) Sheldrick, G. M. *Acta Crystallogr., Sect. A: Found. Crystallogr.* **1990**, *46*, 467−473.
(80) *ORTEP, TEXSAN Structure Analysis Package*; Molecular Structure Corp.: The Woodlands, TX, 1999.

DOI: 10.1021/acs.organomet.7b00432
Organometallics XXXX, XXX, XXX−XXX